

# Origin of the black-golden transition in $\text{Sm}_{1-x}\text{Y}_x\text{S}$

Keiichiro Imura<sup>1</sup>, Mai Saito<sup>1</sup>, Masaki Kaneko<sup>2</sup>, Takahiro Ito<sup>2,3</sup>,  
Tetsuya Hajiri<sup>2</sup>, Masaharu Matsunami<sup>4,5</sup>, Shin-ichi Kimura<sup>4,5,7</sup>,  
Kazuhiko Deguchi<sup>1</sup>, Hiroyuki S. Suzuki<sup>6</sup>, Noriaki K. Sato<sup>1</sup>

<sup>1</sup>Graduate School of Science, Nagoya University, Nagoya 464-8602, Japan

<sup>2</sup>Graduate School of Engineering, Nagoya University, Nagoya 464-8603, Japan

<sup>3</sup>Nagoya University Synchrotron Radiation Research Center, Nagoya University, Nagoya 464-8602, Japan

<sup>4</sup>UVSOR Facility, Institute for Molecular Science, Okazaki 444-8585, Japan

<sup>5</sup>School of Physical Sciences, The Graduate University for Advanced Studies (SOKENDAI), Okazaki 444-8585, Japan

<sup>6</sup>Quantum Beam Center, National Institute for Materials Science, Tsukuba 305-0047, Japan

E-mail: imura@mlab2.phys.nagoya-u.ac.jp

## Abstract.

We report angle-resolved photoemission spectroscopy, electrical resistivity and Hall effect measurements on  $\text{Sm}_{1-x}\text{Y}_x\text{S}$ . At the smallest doping concentration  $x = 0.03$ , the system changes from a semiconducting to metallic conductivity, whereas it is at a critical concentration  $x_c \simeq 0.19$  that there occurs the volume collapse accompanied by a color change from black to golden. It appears that the band gap between  $4f$  and  $5d$  bands vanishes at  $x_c$ . From these results, we suggest that the black-to-golden transition of  $\text{Sm}_{1-x}\text{Y}_x\text{S}$  has the same mechanism as the pressure-induced valence transition of SmS, but the semiconductor-to-metal transition has a different origin for  $\text{Sm}_{1-x}\text{Y}_x\text{S}$  and SmS.

## 1. Introduction

Samarium mono-sulfide (SmS) is well known to exhibit successive phase transitions under pressure; a valence transition called the black-golden (BG) transition at a first critical pressure  $P_{c1}$  ( $\sim 0.65$  GPa at room temperature) from a semiconducting phase (“black phase”) to a valence-fluctuating metallic phase (“golden phase”) [1], and a magnetic phase transition at a second critical pressure  $P_{c2}$  ( $\sim 1.8$  GPa at low temperature) from a paramagnetic to antiferromagnetically ordered state [2, 3, 4]. In spite of intensive experimental and theoretical studies, the mechanism of the BG transition is not well understood yet. Photoemission spectroscopy (PES), especially angle-resolved photoemission spectroscopy (ARPES), is a useful technique to study such a transition, but not available under pressure. To avoid this difficulty, we measure an alloy system  $\text{Sm}_{1-x}\text{Y}_x\text{S}$  that shows a phase transition mimic to the BG transition at ambient pressure [5]. In our previous paper, we studied  $\text{Sm}_{1-x}\text{Y}_x\text{S}$  with  $x = 0$  and  $0.33$  using the ARPES technique and reported that an intermediate-valence state of Sm ion emerges at  $x = 0.33$  [6]. In the present study, we report a detailed study on  $\text{Sm}_{1-x}\text{Y}_x\text{S}$  with  $x = 0.03, 0.12$

<sup>7</sup> present address: Graduate School of Frontier Biosciences and Physics Department, Osaka University, Osaka 565-0871, Japan



and 0.32 to clarify the relationship between the valence transition and a semiconductor-to-metal transition.

## 2. Experimental technique

A single crystal growth was carried out using high-purity starting materials (99.99%-pure (4N) Sm-chips, 5N Y-chips and 6N S-grains) in terms of a high-frequency induction furnace [6]. A lattice constant of the obtained single crystals was determined by X-ray diffraction (XRD) measurements using Cu  $K\alpha$  radiation. The yttrium concentration  $x$  was determined using an inductively-coupled-plasma atomic-emission spectroscopy (ICP-AES) technique. The electrical resistivity and the Hall effect were measured by using a conventional direct current 4-probe method. Magnetic-field is applied by using a superconducting magnet up to 15 T. ARPES measurements were performed at the VUV-ARPES beamline BL5U of UVSOR-III, Institute for Molecular Science [7]. The energy resolution of  $h\nu/\Delta E \sim 1000$  was estimated by measuring a Fermi edge of a polycrystalline gold sample at  $T = 10$  K. The base pressure of the ARPES main chamber was about  $1 \times 10^{-8}$  Pa and a clean (001) surface of  $\text{Sm}_{1-x}\text{Y}_x\text{S}$  was obtained by an *in situ* cleaving method at 10 - 20 K just before the measurement.

## 3. Results and Discussion

Figure 1 shows the lattice constant of  $\text{Sm}_{1-x}\text{Y}_x\text{S}$  as a function of the yttrium concentration  $x$ . With increasing  $x$  from 0 to 0.15, the lattice constant decreases monotonically from 5.97 to 5.86 Å. At a critical concentration  $x_c$ , it shows a discontinuous drop. We note that this first-order transition with a volume collapse of about 3% is accompanied by a color change from black to golden and therefore interpreted as the BG transition. With further increasing  $x$  in the golden phase  $x > x_c$ , the lattice constant decreases again from 5.71 Å at  $x = 0.23$  to 5.5 Å at  $x = 1.0$ , the latter corresponding to the non-doped end-material YS.

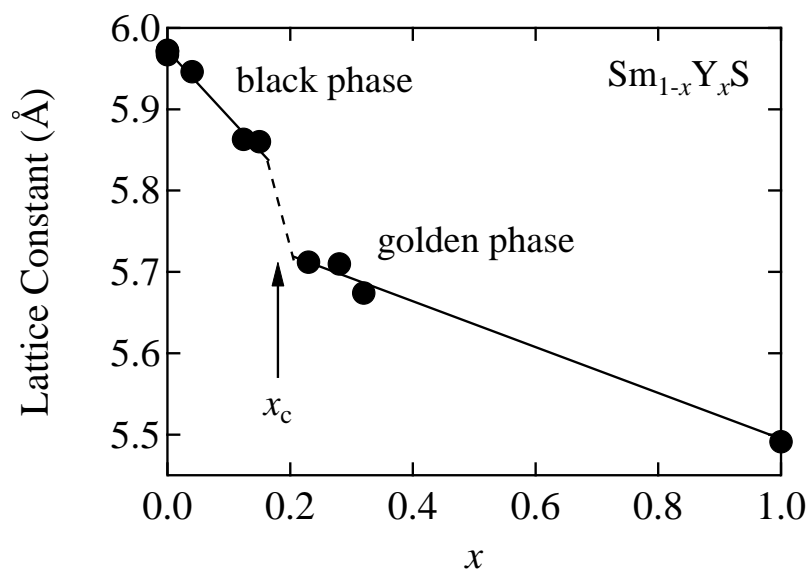


**Figure 1.** Yttrium concentration ( $x$ ) dependence of the lattice constant of  $\text{Sm}_{1-x}\text{Y}_x\text{S}$ . The concentration is evaluated from the ICP-AES analysis.  $x_c$  ( $\sim 0.19$ ) is a critical concentration of the black-golden transition.

Figure 2(a) shows the temperature dependence of the electrical resistivity  $\rho(T)$  of non-doped SmS (i.e.,  $x = 0$ ). As seen from an exponentially steep increase, SmS shows an activation-type

temperature dependence of the electrical resistivity. An energy gap of about 1000 K is an indirect gap between the top of Sm-4*f* derived valence bands at the  $\Gamma$  point in the Brillouin zone (BZ) and the bottom of Sm-5*d* derived conduction bands at the X point [8, 9]. In the inset of Fig. 2(a), the electrical resistivity at room temperature is plotted as a function of  $x$ . With increasing  $x$  from 0 to 0.03, the room-temperature resistivity drops by nearly two orders of magnitude. When further increasing  $x$ , the room-temperature resistivity monotonically decreases possibly due to the increase of the carrier concentration in the conduction band (see below).

In Fig. 2(b), we present the electrical resistivity as a function of temperature for  $x = 0.03$ , 0.12 and 0.32. We find a metallic temperature-dependence of the electrical resistivity even in the smallest composition ( $x = 0.03$ ) sample, meaning that the semiconductor-to-metal transition occurs at a concentration less than 0.03. Note that this critical concentration is much less than the BG transition  $x_c$ . We also observe a residual resistivity to exceed  $250 \mu\Omega\text{cm}$  for  $x = 0.03$ , which we ascribe to a small carrier concentration doped into the conduction band (see below). At  $x = 0.12$ , the resistivity also shows a monotonic decrease with a residual resistivity less than  $100 \mu\Omega\text{cm}$ . The decrease in the residual resistivity with increasing  $x$  is possibly due to an increase of the doped carrier. With increasing  $x$  to 0.32 in the golden phase, the electrical resistivity further decreases. We note that in the pressure-induced golden phase in non-doped SmS [10], the electrical resistivity is non-metallic. The difference in the resistivity between SmS and  $\text{Sm}_{1-x}\text{Y}_x\text{S}$  is ascribed to the fact that the carrier is doped into the conduction band by alloying for  $\text{Sm}_{1-x}\text{Y}_x\text{S}$ .

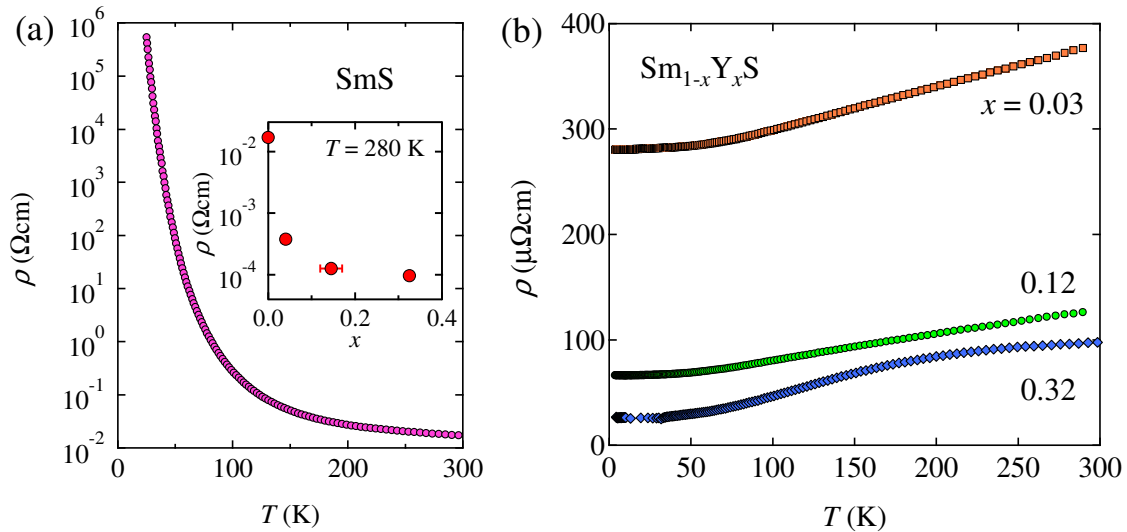


**Figure 2.** Temperature dependence of the electrical resistivity  $\rho$  of pure SmS (a), and  $\text{Sm}_{1-x}\text{Y}_x\text{S}$  ( $x = 0.03$ , 0.12 and 0.32) (b). Inset of (a) shows yttrium concentration dependence of the resistivity at 280 K. The difference between the nominal composition and that deduced from the ICP experiments is denoted by error bar.

Figure 3(a) represents the magnetic-field dependence of the Hall resistivity measured at 2 K for  $\text{Sm}_{1-x}\text{Y}_x\text{S}$  with  $x = 0.03$ , 0.12 and 0.32. For a sample of  $x = 0.03$ , the absolute value of the Hall resistivity increases linearly with magnetic-field. A negative slope of the Hall resistivity curve indicates that the dominant charge carrier is an electron, and the magnitude of the slope (i.e., Hall constant) leads us to evaluate the carrier concentration as 0.015 per formula unit of  $\text{Sm}_{1-x}\text{Y}_x\text{S}$  assuming a single carrier model. With increasing the composition  $x$  to 0.12, the magnitude of the Hall constant becomes smaller with the slope kept negative. The carrier

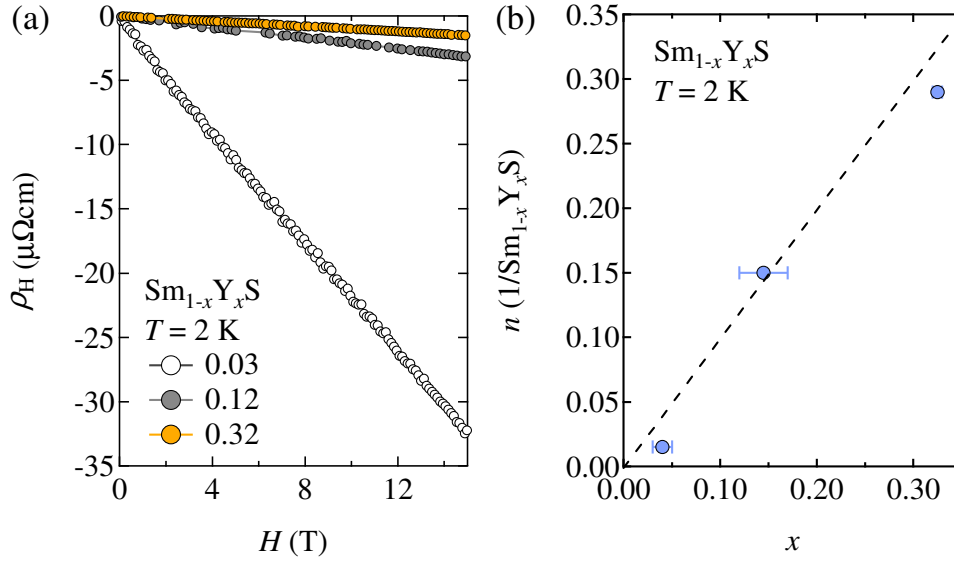


**Figure 3.** (a) Magnetic-field dependence of the Hall resistivity of  $\text{Sm}_{1-x}\text{Y}_x\text{S}$  ( $x = 0.03, 0.12$  and  $0.32$ ) in magnetic fields up to 15 T measured at 2 K. (b) Yttrium concentration  $x$  dependence of the carrier density  $n$  per formula unit of  $\text{Sm}_{1-x}\text{Y}_x\text{S}$  ( $x = 0.03, 0.12$  and  $0.32$ ) at 2 K. Note that  $n$  is estimated by assuming a single band model. The broken line indicates a relationship of  $n = x$ .

concentration at 2 K is evaluated as 0.15 per formula unit. These are qualitatively consistent with the ARPES experiment; there emerges an electron pocket with a light electron-mass near the X point [11]. At the present stage, it is unclear if the volume of the electron pocket is consistent with the carrier concentration deduced from the Hall effect measurement. At  $x = 0.32$  (in the volume-collapsed phase of  $\text{Sm}_{1-x}\text{Y}_x\text{S}$ ), the Hall constant remains negative at low temperature, i.e., the charge carrier remains to be an electron, and the carrier density is evaluated as 0.29 per formula unit of  $\text{Sm}_{1-x}\text{Y}_x\text{S}$  assuming the single band model. The Hall constant of this sample is almost independent of temperature up to 100 K (not shown here).

Previously, we reported that in the golden phase of non-doped SmS, the Hall constant is positive in sign and increases drastically in magnitude with lowering temperature [10]. The upper limit of the carrier density at  $T = 2$  K was evaluated as  $n \sim 3 \times 10^{-3}$  per formula unit assuming a compensated-carrier model. This low-temperature value is two orders of magnitude smaller than that at room-temperature. This indicates that the carrier density decreases with lowering temperature, which we ascribe the pseudo-gap formation.

Figure 3(b) shows the carrier density  $n$  at 2 K as a function of the yttrium concentration  $x$ . We find the almost linear relationship,  $n \sim x$ , which indicates that the substitution of Y for Sm supplies one electron per Y atom into the conduction bands.

Combining these transport properties, we conclude that the golden phase of  $\text{Sm}_{1-x}\text{Y}_x\text{S}$  differs from the golden phase of SmS; while the charge carrier is compensated in the latter, the electron density is larger than the hole density in the former due to the carrier doping effect.

Figure 4 shows the energy distribution curves (EDCs) at the  $\Gamma$  point in the BZ of  $\text{Sm}_{1-x}\text{Y}_x\text{S}$  ( $x = 0, 0.03, 0.12$  and  $0.32$ ) measured at 10 K; some of the results were reported elsewhere [6, 11]. For the non-doped ( $x = 0$ ) sample of SmS, we observe peak structure of bulk origin in the binding energy ranging from 0.5 to 3 eV. (Note that the peak structure of the surface state is denoted by broken line.) This corresponds to a multiplet structure of the  $\text{Sm}^{3+}$  final state ( $^6H$ ,  $^6F$  and  $^6P$ ) through a photoemission process ( $4f^6 + h\nu \rightarrow 4f^5 + e^-$ ) from the initial state of the  $\text{Sm}^{2+}$

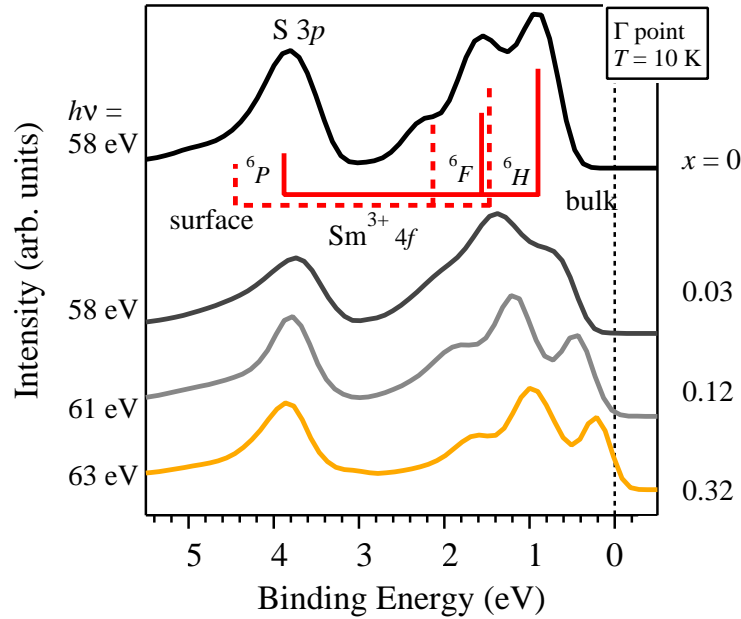


**Figure 4.** Energy distribution curves (EDCs) at the  $\Gamma$  point in the Brillouin zone of  $\text{Sm}_{1-x}\text{Y}_x\text{S}$ . Some of the results were reported elsewhere [6, 11]. In order to investigate the same symmetry point of the several samples which have a different lattice constant, we applied different photon energies. The photon energies ( $h\nu$ ) are shown in the left side of the panel. The solid and broken lines show the multiplet structures of  $\text{Sm } 4f^5$  final state ( $^6H$ ,  $^6F$ ,  $^6P$ ) of bulk and surface states, respectively. The broad peak observed at  $\sim 4$  eV originates from a dispersive S  $3p$  band.

ground state ( $^7F$ ). A peak at 4 eV corresponds to a dispersive S-derived  $3p$  band.

At the  $\Gamma$  point, the spectrum for  $x = 0$  has no amplitude at the Fermi level  $E_F$ . The similar feature is observed at the X point (not shown here). This means that there exists an energy gap between the  $4f$ - and conduction-bands. Note that the  $4f$  bands are almost non-dispersive according to a band structure calculation [9]. For  $x = 0.03$  (in the black phase), we find the energy gap to shrink. It is unclear if the gap closes at  $x = 0.12$ , but the gap is evidently vanished at  $x = 0.32$  (in the golden phase).

Let us discuss a possible origin of the semiconductor-to-metal “transition” and the BG transition of  $\text{Sm}_{1-x}\text{Y}_x\text{S}$ . At  $x = 0$  (i.e.,  $\text{SmS}$ ), the system is a band insulator. The substitution of Y for Sm dopes a charge carrier into the conduction bands formed by the Sm  $5d$  orbitals, as suggested by the negative Hall coefficient. This results in a transformation from the semiconducting to metallic conductivity. When increasing  $x$  beyond the critical concentration  $x_c \sim 0.19$ , the volume collapses as shown in Fig. 1. At  $x = 0.32$ , the multiplet structure of Sm  $4f^5$  final state clearly touches the Fermi level  $E_F$ . Unfortunately, the ARPES data of  $x$  just above  $x_c$  are not available at present. Nevertheless, these results suggest that the BG transition occurs at  $x = x_c$  as a result of the collapse of the band gap between the  $4f$  and  $5d$  bands. This explains that the BG transition is accompanied by a discontinuous valence change from divalence to mixed-valence of Sm ions. In other words, the local  $4f$  electron acquires an itinerant character above  $x_c$ .

According to a very recent high-resolution X-ray absorption spectroscopy (XAS) experiment, the pressure-induced BG transition of pure  $\text{SmS}$  is induced by the promotion of a Sm  $4f$  electron into the  $5d t_{2g}$  band [12]. This means that the BG transition has the same origin for both  $\text{SmS}$  and  $\text{Sm}_{1-x}\text{Y}_x\text{S}$ .

#### 4. Conclusion

We carried out the angle-resolved photoemission spectroscopy, electrical resistivity and Hall effect measurements on the alloying system  $\text{Sm}_{1-x}\text{Y}_x\text{S}$ . At  $x = 0$ , the system (i.e., SmS) is an ionic crystal and a narrow-gap semiconductor with a band gap of the order of  $10^3$  K. At the smallest doping concentration  $x = 0.03$ , the system changes from a semiconducting to metallic conductivity. We observe that at a critical concentration  $x_c \simeq 0.19$ , there occurs the volume collapse accompanied by a color change from black to golden. It appears that the band gap between  $4f$  and  $5d$  bands vanishes at  $x_c$ . From these results, we suggest that the black-to-golden transition of  $\text{Sm}_{1-x}\text{Y}_x\text{S}$  has the same mechanism as the pressure-induced valence transition of SmS, but the semiconductor-to-metal transition has a different origin for  $\text{Sm}_{1-x}\text{Y}_x\text{S}$  and SmS.

#### Acknowledgement

Part of this work was performed by the Use-of-UVSOR Facility program (BL5U, 24-527) of the Institute for molecular Science. This work was partially supported by a grant-in-aid for Scientific Research from JSPS, KAKENHI (No. 20224015).

#### References

- [1] Jayaraman A, *et al.* 1970 *Phys. Rev. Lett.* **25** 1430
- [2] Barla A, *et al.* 2004 *Phys. Rev. Lett.* **92** 066401
- [3] Haga Y, *et al.* 2004 *Phys. Rev. B* **70** 220406
- [4] Matsubayashi K, *et al.* 2007 *Physica B* **310** 408
- [5] Tao L J and Holtzberg F, 1975 *Phys. Rev. B* **11** 3842
- [6] Imura K, *et al.* 2013 *J. Kor. Phys. Soc.* **62** 2028
- [7] Ito T, *et al.* 2007 *AIP Conf. Proc.* **879** 587
- [8] Mizuno T, *et al.* 2008 *J. Phys. Soc. Jpn* **77** 113704
- [9] Antonov V N, *et al.* 2002 *Phys. Rev. B* **66** 165208
- [10] Imura K, *et al.* 2011 *J. Phys. Soc. Jpn* **80** 113704
- [11] Kaneko M, *et al.* 2014 *JPS Conf. Proc.* **3** 011080
- [12] Jarrige I, *et al.* 2013 *Phys. Rev. B* **87** 115107